HHS Public Access

Author manuscript

J Am Chem Soc. Author manuscript; available in PMC 2019 September 05.

Published in final edited form as:

J Am Chem Soc. 2018 September 05; 140(35): 11058–11066. doi:10.1021/jacs.8b05814.

Genetically Encoding Quinoline Reverses Chromophore Charge and Enables Fluorescent Protein Brightening in Acidic Vesicles

Caiyun Fu[†,⊥], **Tomonori Kobayashi**[†], **Nanxi Wang**[†], **Christian Hoppmann**[†], **Bing Yang**[†], **Roshanak Irannejad**[‡], and **Lei Wang**[†,‡,*]

[†]Department of Pharmaceutical Chemistry and University of California, San Francisco, San Francisco, California, USA.

[‡]Cardiovascular Research Institute, University of California, San Francisco, San Francisco, California, USA.

[⊥]College of Life Sciences, Zhejiang Sci-Tech University, Hangzhou, China.

Abstract

Acidic vesicles and organelles play fundamental roles in a broad range of cellular events such as endocytosis, lysosomal degradation, synaptic transmission, pathogen fate, and drug delivery. Fluorescent reporters will be invaluable for studying these complex and multifunctional systems with spatiotemporal resolution, yet common fluorescent proteins are generally non-fluorescent at acidic conditions due to the decrease of anionic chromophore upon protonation, but are fluorescent at physiological pH creating interfering fluorescence from non-vesicle regions. Here we developed a novel abFP (acid brightening fluorescent protein) that fluoresces strongly at acidic pH but is non-fluorescent at or above neutral pH, boasting a pH profile opposite to that of common fluorescent proteins. Through expansion of the genetic code, we incorporated a quinoline-containing amino acid Qui into the chromophore of EGFP to reverse the chromophore charge. Protonation of Qui rendered a cationic chromophore, which resulted in unique fluorescence increase only at acidic pH *in vitro*, in *E. coli* cells, and on mammalian cell surface. We further demonstrated that abFP tagged δ opioid receptors were fluorescently imaged in lysosome showing distinct features and without background fluorescence from other cellular regions, whereas EGFP tagged receptors were invisible in lysosome. This Qui-rendered cationic chromophore strategy may be generally applied to other fluorescent proteins to generate a palette of colors for acidic imaging with minimal background, and these abFPs should facilitate the study of molecules in association with various acidic vesicles and organelles in different cells and model organisms.

TOC graphics

Correspondence to: Caiyun Fu; Tomonori Kobayashi.

*To whom correspondence should be addressed: Lei.Wang2@ucsf.edu.

Associated Content

Supporting Information. The Supporting Information is available free of charge on the ACS Publications website. It contains experimental details for chemical synthesis of Qui, plasmid construction, protein expression and purification, mass spectrometry, fluorescence spectrometry, mammalian cell culture, FACS analysis, cell viability assay, and fluorescence microscopy. Figures S1-S5 are also included.

Notes

The authors declare no competing financial interest.

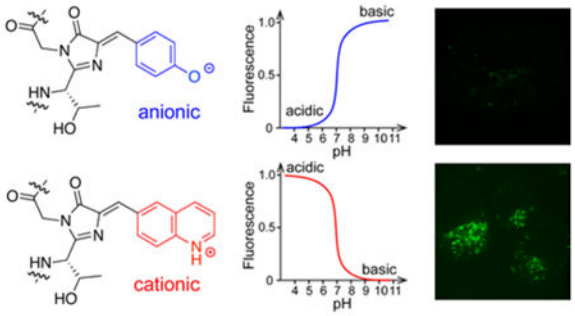

Introduction

Eukaryotic cells have multiple intracellular organelles and vesicles that have an acidic lumen, such as endosomes, lysosomes, autophagosomes, trans-Golgi compartments, and synaptic vesicles[1]. They participate in endocytosis and/or exocytosis, playing fundamental roles in a broad range of cellular events. For instance, endocytic trafficking via endosomes delivers membrane components, receptor-associated ligands and solute molecules to various intracellular destinations[2]; lysosomes degrade and recycle cellular waste, and are further involved in secretion, plasma membrane repair, nutrient signaling and energy metabolism[3]; synaptic vesicle release is a fundamental step in inter-neuronal signaling[4]. These complex itineraries also control the intracellular fates of pathogens and toxins, and determine the intracellular targeting of therapeutic agents[5]. The dysfunction of any of these pathways often leads to various diseases. It is thus of fundamental importance to understand the complex and multifunctional roles of these vesicles and organelles.

Fluorescence microscopy provides spatial-temporal resolution and has been invaluable for studying dynamic cellular processes in live cells. For investigating acidic vesicles, it would be ideal to have fluorescent indicators that are non-fluorescent at physiological pH 7.4 and become fluorescent at acidic intra-vesicular pH values. Such indicators will brighten up in acidic vesicles only, clearly distinguish vesicles of interest from other cellular structures and regions. Small molecule fluorescent indicators with such pH response have been developed recently for visualizing exocytosis[6,7]. Although valuable, small molecule probes lack genetic specificity in general. A genetically encoded indicator would allow precise targeting to organelle, compartment or tissue, selectively appending to specific proteins, stable expression for study over time, and noninvasive imaging to minimize perturbation. Fluorescent proteins (FPs) are genetically encoded and have been engineered to sense pH change for reporting of vesicles[8–11]. Nonetheless, monomeric FPs and their derived pH indicators are generally non-fluorescent at acidic pH and become fluorescent when pH is shifted to the physiological pH[12]. This pH response profile is suitable for detecting events that expose vesicle contents to the higher neutral pH, but is incapable of visualizing intra-vesicular contents, resting vesicles, and intracellular vesicle dynamics, due to indicator's invisibility in acidic conditions and high background fluorescence at non-vesicle regions.

Here we report the development of an abFP (*a*cid *b*rightening *F*luorescent *P*rotein) possessing a pH profile contrary to common FPs. Through genetic code expansion,

quinonine was genetically incorporated into the chromophore of GFP to sense pH change via a unique, positively charged chromophore. The resultant abFP is invisible at and above physiological pH but brightly fluoresces at acidic pHs. By fusing abFP to target receptors, we demonstrated the clear imaging of ligand-induced endocytosis opioid receptors with distinct fluorescence at lysosomes and no background fluorescence of other cellular structures. We expect that the unique fluorescence of abFP at acidic conditions will markedly expand the optical investigation of various acidic vesicles previously invisible to optical microscopy.

Results

Design a quinoline-based chromophore to sense pH change

The chromophore of most FPs consists of a tyrosine residue, the phenol group of which shifts its protonation-deprotonation equilibrium in response to pH (Fig. 1a). When pH changes to acidic values, the phenolate species will decrease, and thus excitation of the corresponding anionic chromophore leads to decrease of fluorescence intensity, resulting in a profile of pH response typical for common FPs shown in Fig. 1b.

Instead of relying on an anionic chromophore, we reasoned whether introduction of a positive charge onto the chromophore would reverse the pH profile, as acidic pH will shift equilibrium toward the positively charged chromophore. We decided to use quinoline, because it has ideal pKa values (pKa 5~6) at the nitrogen atom in the conjugated ring for protonation, which are suitable for detecting physiological pH changes in acidic organelles and vesicles. Another important consideration is that after incorporating quinoline into the chromophore the resultant FP should maintain its strong fluorescence. Most reported FPs have a heteroatom (oxygen or nitrogen) at the phenol position in the chromophore[13]; using unnatural amino acid (Uaa) mutagenesis we previously showed that GFP mutants without a heteroatom at the phenol position significantly lost their fluorescence[14]. Therefore, we designed a quinoline-containing Uaa (L-β-(quinolin-6-yl) alanine, Qui) with a nitrogen atom at the *para* position of the -β-carbon (Fig. 1c). Through the expansion of the genetic code[15–17], we could evolve an orthogonal tRNA/synthetase pair to site-specifically incorporate the designed Qui into FP in live cells, expecting that the chromophore with Tyr substituted by Qui would similarly form and fluoresces. As Qui can equilibrate between protonation and deprotonation with a positive charge, we expect the pH profile of the Qui-containing FP would show an opposite trend from that of common FPs (Fig. 1d).

Genetically incorporate Qui into proteins in *E. coli*

Qui was synthesized using a palladium-catalyzed cross-coupling method with N^{α}-*tert*-butyloxycarbonyl (Boc)-L-β-iodoalanine methyl ester and 6-bromoquinoline followed by acidic deprotection of the Boc group and the methyl ester (see Supplementary Information)[18].

To genetically incorporate Qui into proteins, we initially tried the *Methanosarcina mazei* (Mm) $tRNA^{Pyl}$ together with MmNapRS, an aminoacyl-tRNA synthetase evolved from MmPylRS for specific incorporation of L-3-(2-naphthyl)alanine (Nap, Fig. 2a) in response

to the amber stop codon (TAG)[19]. Although Qui was structurally similar to Nap, we found that $tRNA^{Pyl}$/MmNapRS could not incorporate Qui into proteins possibly due to the electrostatic effect of the nitrogen atom on the quinoline ring. We then decided to evolve the $tRNA^{Pyl}$/MmPylRS pair to be specific for Qui. We have reported the generation of multiple MmPylRS mutants specific for bulky phenylalanine analogues substituted with a benzoyl group[19], an azobenzene group[20] and long alkyl halide groups[21]. Based on these experiences, we created a mutant library of MmPylRS with five residues (N346, C348, V401, W417, and G419) saturatedly mutated and then subjected to selections as described[22,23]. One mutant, named as MmQuiRS, was identified from the selection to afford Qui-dependent phenotype (Fig S1). The amino acid sequences in the active site of MmQuiRS were markedly different from those of MmNapRS and MmPylRS (Fig. 2b, 2c.

We evaluated the incorporation specificity of Qui into proteins in *E. coli*. The gene for the enhanced green fluorescent protein (EGFP) containing a TAG codon at site 182 (EGFP-182TAG, a permissive and non-chromophore forming residue) was co-expressed with the $tRNA^{Pyl}$/MmQuiRS pair in *E. coli*. In the absence of Qui, no full-length EGFP was detected; when 1 mM Qui was added in growth media, full-length EGFP was produced (Fig. 2d) in the yield of 3.5 mg/L. The purified EGFP-182Qui was analyzed by electrospray ionization time-of-flight mass spectrometry (ESI-TOF MS) (Fig. 2e). A peak observed at 27967.2 Da corresponds to the intact EGFP with Qui at the position 182 (EGFP182Qui: expected 27967.8 Da); another peak observed at 27836.4 Da corresponds to the EGFP182Qui lacking the initiator Met (EGFP182Qui-Met: expected 27836.6 Da). No peaks corresponding to misincorporation of natural amino acids at the 182TAG position was identified. These results indicate that the evolved $tRNA^{Pyl}$/MmQuiRS pair was able to incorporate Qui with high efficiency and specificity in *E. coli*.

Develop Qui-based abFP

To utilize Qui for pH sensing, we then incorporated Qui at position 66 of EGFP to replace the chromophore forming Tyr residue (Fig. 3a). EGFP-66TAG gene was co-expressed with the $tRNA^{Pyl}$/MmQuiRS pair in *E. coli*. In the presence of 1 mM Qui in growth media, full-length EGFP protein was produced (Fig. 3b). The purified EGFP-66Qui protein was analyzed by ESI-TOF MS (Fig. 3c). A peak at 27967.6 Da was observed, corresponding to intact EGFP containing Qui at site 66 (EGFP66Qui: expected 27967.8 Da); the EGFP66Qui lacking the initiator Met was also observed at 27836.6 Da (expected 27836.6). These data support that Qui was specifically incorporated at the desired position 66 of EGFP, and that the chromophore was formed correctly in a similar manner as the EGFP.

To characterize the fluorescence property of EGFP-66Qui, we first measured the absorption spectra of the purified protein in the neutral phosphate buffer (Fig. 3d). EGFP (EGFP66Tyr) has a major absorption peak at 488 nm, while EGFP-66Qui had a major absorption peak at 385 nm, and only small absorption was measured around 475 nm. Since 385 nm is in the UV region and not appropriate for live cell imaging, fluorescence emission spectra of EGFP-66Qui were then measured in aqueous buffers with different pH at 475 nm excitation (Fig. 3e). Fluorescence emission peaked at 510 nm, and the intensity changed in response to pH variation. Upon pH change from acidic (pH 4.4) to neutral (pH 7.4) condition, the

fluorescence intensity increased by 8-fold. The pKa value for fluorescence change was determined as 5.7 (Fig. 3f), which corresponds well to the reported pKa value of quinoline, supporting that fluorescence intensity change of EGFP-66Qui in response to pH was due to Qui. Although EGFP-66Qui showed pH-responsive fluorescence change, its pH profile remained similar to common FPs.

During experimentation we unexpectedly found that the EGFP-66Qui protein solution changed from colorless to light red after keeping it under the ambient light for a while. This observation prompted us to check if EGFP-66Qui was photoactivatible. We thus illuminated a fresh EGFP-66Qui protein prepared in dark with 365-nm light, and indeed found that the sample turned red within several minutes (Fig. 4a). After illumination, its absorption spectrum changed correspondingly, with absorption maxima shifted from 385 nm to 523 nm in phosphate buffer (pH 7.4) (Fig. 4b). We next measured fluorescence emission spectra of the photoproduct in aqueous buffers of different pH. When excited at 475 nm, a wavelength between the two absorption peaks, the photoactivated EGFP66Qui showed ratiometric spectral change (Fig. 4c). From pH 5.8 to pH 9.0, the main fluorescence emission maxima were measured at ~510 nm; when pH was shifted to more acidic values (5.6 to 3.8), the fluorescence emission maxima were red-shifted to 566–582 nm. More excitingly, the fluorescence intensity of the peak around 570 nm increased upon pH change from neutral (pH 7.4) to acidic (pH 3.8). The pKa value for fluorescence change was determined as 5.2 (Fig. 4d) and well corresponded to that of quinoline, suggesting that the incorporated Qui still worked as the pH sensing unit after photoactivation. It was amazing to observe that the photoactivated EGFP66Qui was able to fluoresce strongly at the extreme acidic pH 3.8, a property that hasn't been reported for other FPs. Meanwhile, the photoactivated EGFP66Qui was almost non-fluorescent at the physiological pH 7.4 at ~570 nm, which will be invaluable for reducing background fluorescence; its weak fluorescence at 510 nm at pH 7.4 will be helpful for localization of the labeled target. The extinction coefficient and quantum yield of the photoactivated EGFP66Qui were measured at pH values 7.4, 5.6, and 4.6 (Fig. 4e). When shifted from pH 7.4 to acidic pH, its brightness increased 450-fold at pH 5.6 and 713-fold at pH 4.6, respectively. Therefore, the photoactivated EGFP-66Qui presents a desired pH profile of fluorescence that is inverse to common FPs and capable of covering the whole acidic pH range encountered in live cells. We thus named EGFP-66Qui as abFP for its ability to brighten up in acidic conditions after photoactivation.

Wild type GFP has been reported to photoconvert from the 398 nm-absorbing state (neutral chromophore) to the 475 nm-absorbing state (anionic chromophore) upon illumination, with a concomitant decarboxylation of residue Glu222[24]. Glu222 locates close to and participates in the hydrogen bonding network with the chromophore. To probe possible structural change underlying the photoactivation of EGFP-66Qui, we analyzed the protein sample after UV illumination using ESI-TOF MS. Amazingly, two peaks were observed corresponding exactly to the loss of 44 Da (mass of CO_2) from the two peaks of the EGFP-66Qui before illumination, suggesting decarboxylation of Glu222 as well (Fig. 4f). Specifically, a peak observed at 27923.8 Da corresponds to the decarboxylation of EGFP-66Qui (EGFP66Qui-CO_2: expected 27923.8 Da); the other peak observed at 27792.7 Da corresponds to the decarboxylation of EGFP-66Qui lacking the initiating Met (EGFP66Qui-Met-CO_2: expected 27792.6 Da). We further digested the photoactivated EGFP-66Qui with trypsin and then

analyzed using tandem MS. A series of b and y ions unambiguously indicate that the decarboxylation occurred at the Glu222 residue (Fig. 4g).

To quickly check abFP's ability to sense pH in live cells, we expressed abFP in *E. coli* cells and treated the pelleted cells with or without photoactivation by 365 nm light. The external media were then exchanged to buffers of pH 7.4 or 4.4, and the pelleted cells were excited at 470±20 nm and photographed through a 530 nm long pass filter. Strong yellow fluorescence was observed only from cells in the pH 4.4 buffer after photoactivation (Fig. 4h). These data suggest that abFP can work as a photoactivatable pH indicator in living bacterial cells.

Genetically incorporate Qui into proteins in mammalian cells

To enable the usage of abFP in mammalian cells, we began by testing and optimizing the incorporation of Qui into proteins in mammalian cells. A HeLa-EGFP-182TAG reporter cell line was used, which has the EGFP gene containing the TAG amber stop codon at the permissive site 182 stably integrated into the genome[25]. Suppression of this 182TAG codon by incorporating the tested Uaa will result in full-length EGFP rendering HeLa cells green fluorescent. Plasmid pMP-QuiRS-1xtRNA or pMP-QuiRS-3xtRNA, encoding the MmQuiRS and indicated copies of $tRNA^{Pyl}$, was transfected in the reporter cells. After transfection, cells were incubated with Qui of various concentrations at 37 °C for 24 or 48 h followed by flow cytometry. Strong EGFP fluorescence was measured from cells when Qui was added (Fig. 5a, Fig S2). The fluorescence intensity increased with Qui concentration, tRNA copy, and Qui incubation time (Fig. 5b), indicating the efficient incorporation of Qui into EGFP in HeLa cells. For subsequent experiments in mammalian cells, we used 1 mM Qui, $3xtRNA^{Pyl}$, and 48 h unless indicated otherwise.

Another important consideration for Uaa application in mammalian cells is the potential cytotoxicity of Uaa. We measured the viability of cells incubated with various concentrations of Qui using alamarBlue. Qui did not cause obvious toxicity to HeLa-EGFP-182TAG reporter cells (Fig. 5c) or HeLa cells (Fig S3).

Expression of abFP in mammalian cells to sense acidic pH

We next expressed abFP directly in HeLa cells. To facilitate pH change by using external buffers, we displayed abFP or EGFP on HeLa cell surface by fusing them with human interleukin-2 receptor α-subunit Tac, which resides at the plasma membrane and targets the fused protein to the extracellular side.[26] Plasmids pMP-QuiRS-3xtRNA and pcDNA3.1-EGFP66TAG-Tac were co-transfected into HeLa cells, and the cells were incubated with 1 mM Qui for 48 h. Following photoactivation using 385 nm light, the cells were exposed to buffer with various pH and then imaged. For cells expressing abFP, only faint fluorescence was detected at pH 7.2, but clear and stronger fluorescence were imaged when pH was shifted to the more acidic 5.6, 4.6 and 3.8 (Fig. 6a). In control HeLa cells expressing EGFP, strong green fluorescence was observed at pH 7.2, but the intensity decreased precipitously with pH shifting to 5.6 and 4.6, and became almost invisible at 3.8 (Fig. 6b). The pH profile of abFP fluorescence in HeLa cells is drastically opposite to that of EGFP, consistent with *in vitro* data. Western blot analyses of these cells showed that the expression level of abFP-Tac or EGFP-Tac did not vary significantly with the exposed pH (Fig. S4), indicating that

fluorescence change was not due to the change of protein amount. These microscopic results indicate that abFP was successfully expressed in HeLa cells and able to fluoresce strongly in acidic pH with minimal background fluorescence at physiological pH.

Fluorescence imaging of endocytosed receptors using abFP

Endocytosis is a conserved mechanism for regulating various receptors. Many receptors have been recently discovered to initiate signaling not only from cell surface but also from subcellular locations such as endosomes and Glogi apparatus[27–32]. The ability to clearly image receptors internalized into acidic subcellular structures would facilitate the study of endocytic trafficking of receptors and the emerging 'location bias' of receptor functional selectivity. To demonstrate abFP's ability to light up receptors internalized into the acidic vesicles, we fused abFP or EGFP with the δ opioid receptor (DOR) for fluorescent imaging in mammalian cells. DOR is a subtype of G protein-coupled receptors (GPCRs) that are activated by endogenous opioid neuropeptides and by clinically important opiate drugs. After agonist-induced endocytosis, DOR traffics selectively to lysosomes via endosomes.

We fused abFP or EGFP at the C-terminus of DOR and expressed the receptor in HeLa cells (Fig. 7a). abFP was photo-activated and cells were imaged using fluorescence confocal microscopy. LysoTracker Red, a cell-permeant small molecule probe that selectively accumulates in acidic organelles, was applied to cells for comparison. Before exposure to agonist (t = 0 min), cells expressing DOR-EGFP showed strong green fluorescence, which did not overlap with the red fluorescence of the LysoTracker (Fig. 7b), indicating receptors locating at non-acidic environment. In contrast, cells expressing DOR-abFP had almost no detectable green fluorescence (Fig. 7c), consistent with abFP's extremely low fluorescence intensity at neutral pH 7.4. The cells were then treated with agonist DADLE to stimulate DOR endocytosis. After stimulation for 60 min, cells expressing DOR-EGFP had decreased green fluorescence, which still did not overlap with the red fluorescence of LysoTracker (Fig. 7b). At 90 min, green fluorescence became almost non-detectable from these cells, indicating that DOR receptors had mainly trafficked to lysosome. During the endocytosis process EGFP was unable to fluorescently indicate the DOR receptor at acidic vesicles. In striking contrast, cells expressing DOR-abFP had green fluorescence emerged after agonist stimulation, and accumulated with time (Fig. 7c). In addition, the green fluorescence overlapped extensively with the red fluorescence of the LysoTracker, both appeared in puncta, suggesting that the DOR-abFP receptors were trafficking to lysosome. Moreover, as abFP was almost non-fluorescent at neutral pH, there was no background fluorescence of DOR at non-acidic locations, making the DOR at acidic vesicles highly distinct. The ratio of DOR-xxFP fluorescence intensity to that of LysoTracker measured from these cells clearly indicate that abFP had the opposite trend from EGFP in reporting receptor endocytosis (Fig. 7d). For abFP tagged DORs, their fluorescence ratio increased more than 4-fold after the DOR was endocytosed into the lysosome, providing high signal over noise for imaging and detection. Western blot analyses showed that the protein level of DOR-EGFP or DOR-abFP did not change significantly in the time range (Fig. S5), indicating that the observed fluorescence change was not due to the change of protein amount.

Discussion

The chromophore of common FPs consisting of a Tyr residue can equilibrate between a neutral and anionic state due to protonation and deprotonation of the phenolic hydroxyl group. Compared with the anionic chromophore, the neutral chromophore of FPs usually has shorter excitation wavelength and lower brightness for emission. Therefore, most FPs have been optimized to use the anionic chromophore for fluorescence imaging[11,33]. Previous pH sensitive indicators derived from FPs, such as the ecliptic pHluorin[8], often suppress the neutral chromophore as well. Consequently, FPs are weakly to non-fluorescent in acidic conditions in general due to the decrease of the anionic chromophore[9,12], making them unsuitable for imaging molecules residing in acidic environments. Here we reversed the charge of the chromophore from anionic to cationic by genetically encoding a quinoline-containing unnatural amino acid Qui into the chromophore of EGFP. At acidic pH, Qui is protonated increasingly, shifting the equilibrium of chromophore toward the cationic state and hence increasing the fluorescence intensity. The resultant abFP thus has a pH profile that is opposite to common FPs: abFP is strongly fluorescent in acidic conditions, as low as pH 3.8, and almost nonfluorescent at and above physiological pH 7.4. There are various Tyr-containing FPs covering a broad range of wavelengths; our strategy of replacing the chromophore Tyr with Qui may be generally applied to these FPs to generate a palette of colors for acidic imaging.

The unique pH profile makes abFP especially well-suited for fluorescence imaging of acidic vesicles: being strongly fluorescent inside the acidic vesicles while invisible at other cellular structures to reduce the interfering background fluorescence. Incorporation of the novel Qui into the chromophore red-shifted the fluorescence of the parental EGFP: abFP showed excitation peak of 523 nm (green) and emission at 560–580 nm (orange), which are suitable for live cell imaging. Here we demonstrated the use of abFP to fluorescently image the endocytosed DOR receptors in live mammalian cells, showing distinct fluorescent puncta structures intensively overlapping with the LysoTracker. In addition, abFP is photoactivatible, which may be valuable for *in cellulo* pulse-chase labeling for tracking subpopulations of cells, organelles or proteins, and for super-resolution imaging of single molecules[34]. Moreover, unnatural amino acids have been genetically encoded in mammalian cells, neurons[25], stem cells[35], *C. elegans*[36], zebrafish[37], and mouse[37,38], and our evolved $tRNA^{Pyl}$/MmQuiRS are compatible for use in these systems to incorporate Qui into abFP. Therefore, we expect that abFPs should be useful for studying molecules residing in a variety of acidic vesicles and organelles, which range from endosomes, lysosomes, autophagosomes, trans-Golgi network, to synaptic vesicles, in different cells and model organisms.

Supplementary Material

Refer to Web version on PubMed Central for supplementary material.

Acknowledgments

We gratefully acknowledge Dr. Masanori Funabashi for providing the high-resolution mass spectrometry measurement of Qui, Drs. Jacob Eriksen and Robert Edwards for plasmid pCDNA3.1-scFv-Tac. Support from U.S. National Institutes of Health (RF1MH114079 and R01GM118384 to L.W.) is acknowledged.

References

1. Casey JR, Grinstein S & Orlowski J Sensors and regulators of intracellular pH. Nat. Rev. Mol. Cell Biol 11, 50–61 (2010). [PubMed: 19997129]
2. Maxfield FR & McGraw TE Endocytic recycling. Nat. Rev. Mol. Cell Biol 5, 121–132 (2004). [PubMed: 15040445]
3. Settembre C, Fraldi A, Medina DL & Ballabio A Signals from the lysosome: a control centre for cellular clearance and energy metabolism. Nat. Rev. Mol. Cell Biol 14, 283–296 (2013). [PubMed: 23609508]
4. Sinning A & Hubner CA Minireview: pH and synaptic transmission. FEBS Lett 587, 1923–1928 (2013). [PubMed: 23669358]
5. Rajendran L, Knolker HJ & Simons K Subcellular targeting strategies for drug design and delivery. Nat. Rev. Drug Discov 9, 29–42 (2010). [PubMed: 20043027]
6. Adie EJ, Francis MJ, Davies J, Smith L, Marenghi A, Hather C, Hadingham K, Michael NP, Milligan G & Game S CypHer 5: a generic approach for measuring the activation and trafficking of G protein-coupled receptors in live cells. Assay Drug Dev. Technol 1, 251–259 (2003). [PubMed: 15090190]
7. Asanuma D, Takaoka Y, Namiki S, Takikawa K, Kamiya M, Nagano T, Urano Y & Hirose K Acidic-pH-activatable fluorescence probes for visualizing exocytosis dynamics. Angew. Chem. Int. Ed. Engl 53, 6085–6089 (2014). [PubMed: 24801356]
8. Miesenbock G, De Angelis DA & Rothman JE Visualizing secretion and synaptic transmission with pH-sensitive green fluorescent proteins. Nature 394, 192–195 (1998). [PubMed: 9671304]
9. Shen Y, Rosendale M, Campbell RE & Perrais D pHuji, a pH-sensitive red fluorescent protein for imaging of exo- and endocytosis. J. Cell Biol 207, 419–432 (2014). [PubMed: 25385186]
10. Kneen M, Farinas J, Li Y & Verkman AS Green fluorescent protein as a noninvasive intracellular pH indicator. Biophys. J 74, 1591–1599 (1998). [PubMed: 9512054]
11. Tsien RY Constructing and exploiting the fluorescent protein paintbox (Nobel Lecture). Angew. Chem. Int. Ed. Engl 48, 5612–5626 (2009). [PubMed: 19565590]
12. Lin MZ & Schnitzer MJ Genetically encoded indicators of neuronal activity. Nat. Neurosci 19, 1142–1153 (2016). [PubMed: 27571193]
13. Chudakov DM, Matz MV, Lukyanov S & Lukyanov KA Fluorescent proteins and their applications in imaging living cells and tissues. Physiol. Rev 90, 1103–1163 (2010). [PubMed: 20664080]
14. Wang L, Xie J, Deniz AA & Schultz PG Unnatural amino acid mutagenesis of green fluorescent protein. J. Org. Chem 68, 174–176 (2003). [PubMed: 12515477]
15. Wang L, Brock A, Herberich B & Schultz PG Expanding the genetic code of Escherichia coli. Science 292, 498–500 (2001). [PubMed: 11313494]
16. Wang L & Schultz PG Expanding the genetic code. Angew. Chem. Int. Ed. Engl 44, 34–66. (2005).
17. Wang L Engineering the Genetic Code in Cells and Animals: Biological Considerations and Impacts. Acc. Chem. Res 50, 2767–2775 (2017). [PubMed: 28984438]
18. Jackson RFW & Perez-Gonzalez M Synthesis of N-(tert-butoxycarbonyl)-beta-iodoalanine methyl ester: a useful building block in the synthesis of nonnatural alpha-amino acids via palladium catalyzed cross coupling reactions. Org. Synth 81, 77–88 (2005).
19. Lacey VK, Louie GV, Noel JP & Wang L Expanding the library and substrate diversity of the pyrrolysyl-tRNA synthetase to incorporate unnatural amino acids containing conjugated rings. ChemBioChem 14, 2100–2105 (2013). [PubMed: 24019075]
20. Hoppmann C, Lacey VK, Louie GV, Wei J, Noel JP & Wang L Genetically encoding photoswitchable click amino acids in Escherichia coli and mammalian cells. Angew. Chem. Int. Ed. Engl 53, 3932–3936 (2014). [PubMed: 24615769]

21. Xiang Z, Lacey VK, Ren H, Xu J, Burban DJ, Jennings PA & Wang L Proximity-enabled protein crosslinking through genetically encoding haloalkane unnatural amino acids. Angew. Chem. Int. Ed. Engl 53, 2190–2193 (2014). [PubMed: 24449339]
22. Takimoto JK, Dellas N, Noel JP & Wang L Stereochemical basis for engineered pyrrolysyl-tRNA synthetase and the efficient in vivo incorporation of structurally divergent non-native amino acids. ACS Chem. Biol 6, 733–743 (2011). [PubMed: 21545173]
23. Wang N, Yang B, Fu C, Zhu H, Zheng F, Kobayashi T, Liu J, Li S, Ma C, Wang PG, Wang Q & Wang L Genetically Encoding Fluorosulfate-l-tyrosine To React with Lysine, Histidine, and Tyrosine via SuFEx in Proteins in Vivo. J. Am. Chem. Soc 140, 4995–4999 (2018). [PubMed: 29601199]
24. van Thor JJ, Gensch T, Hellingwerf KJ & Johnson LN Phototransformation of green fluorescent protein with UV and visible light leads to decarboxylation of glutamate 222. Nat. Struct. Biol 9, 37–41 (2002). [PubMed: 11740505]
25. Wang W, Takimoto JK, Louie GV, Baiga TJ, Noel JP, Lee KF, Slesinger PA & Wang L Genetically encoding unnatural amino acids for cellular and neuronal studies. Nat. Neurosci 10, 1063–1072 (2007). [PubMed: 17603477]
26. Tan PK, Waites C, Liu Y, Krantz DE & Edwards RH A leucine-based motif mediates the endocytosis of vesicular monoamine and acetylcholine transporters. J. Biol. Chem 273, 17351–17360 (1998). [PubMed: 9651318]
27. Irannejad R, Tomshine JC, Tomshine JR, Chevalier M, Mahoney JP, Steyaert J, Rasmussen SG, Sunahara RK, El-Samad H, Huang B & von Zastrow M Conformational biosensors reveal GPCR signalling from endosomes. Nature 495, 534–538 (2013). [PubMed: 23515162]
28. Mullershausen F, Zecri F, Cetin C, Billich A, Guerini D & Seuwen K Persistent signaling induced by FTY720-phosphate is mediated by internalized S1P1 receptors. Nat. Chem. Biol 5, 428–434 (2009). [PubMed: 19430484]
29. Calebiro D, Nikolaev VO, Gagliani MC, de Filippis T, Dees C, Tacchetti C, Persani L & Lohse MJ Persistent cAMP-signals triggered by internalized G-protein-coupled receptors. PLoS Biol 7, e1000172 (2009). [PubMed: 19688034]
30. Ferrandon S, Feinstein TN, Castro M, Wang B, Bouley R, Potts JT, Gardella TJ & Vilardaga JP Sustained cyclic AMP production by parathyroid hormone receptor endocytosis. Nat. Chem. Biol 5, 734–742 (2009). [PubMed: 19701185]
31. Tsvetanova NG & von Zastrow M Spatial encoding of cyclic AMP signaling specificity by GPCR endocytosis. Nat. Chem. Biol 10, 1061–1065 (2014). [PubMed: 25362359]
32. Irannejad R, Pessino V, Mika D, Huang B, Wedegaertner PB, Conti M & von Zastrow M Functional selectivity of GPCR-directed drug action through location bias. Nat. Chem. Biol 13, 799–806 (2017). [PubMed: 28553949]
33. Tsien RY The green fluorescent protein. Annu. Rev. Biochem 67, 509–544. (1998). [PubMed: 9759496]
34. Lippincott-Schwartz J & Patterson GH Photoactivatable fluorescent proteins for diffraction-limited and super-resolution imaging. Trends Cell Biol 19, 555–565 (2009). [PubMed: 19836954]
35. Shen B, Xiang Z, Miller B, Louie G, Wang W, Noel JP, Gage FH & Wang L Genetically encoding unnatural amino acids in neural stem cells and optically reporting voltage-sensitive domain changes in differentiated neurons. Stem Cells 29, 1231–1240 (2011). [PubMed: 21681861]
36. Parrish AR, She X, Xiang Z, Coin I, Shen Z, Briggs SP, Dillin A & Wang L Expanding the genetic code of Caenorhabditis elegans using bacterial aminoacyl-tRNA synthetase/tRNA pairs. ACS Chem. Biol 7, 1292–1302 (2012). [PubMed: 22554080]
37. Chen Y, Ma J, Lu W, Tian M, Thauvin M, Yuan C, Volovitch M, Wang Q, Holst J, Liu M, Vriz S, Ye S, Wang L & Li D Heritable expansion of the genetic code in mouse and zebrafish. Cell Res 27, 294–297 (2017). [PubMed: 27934867]
38. Kang JY, Kawaguchi D, Coin I, Xiang Z, O'Leary DD, Slesinger PA & Wang L In vivo expression of a light-activatable potassium channel using unnatural amino acids. Neuron 80, 358–370 (2013). [PubMed: 24139041]

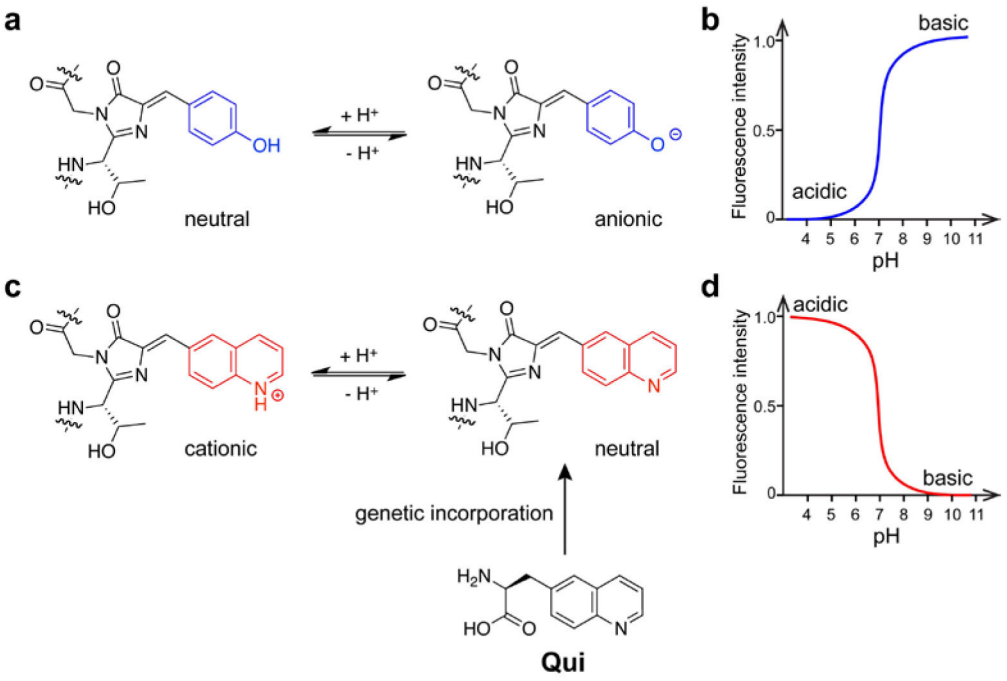

Fig. 1. A quinoline-based chromophore to reverse the pH profile of FP.

a) The chromophore of common FPs contains a Tyr residue, which equilibrates between the neutral phenol and anionic phenolate states in response to pH change. **b**) The profile of fluorescence intensity vs. pH for common FPs, which are usually non-fluorescent at acidic pH values. **c**) Genetically incorporation of Qui in placement of Tyr will create a quinoline-based chromophore, which will equilibrate between a cationic and a neutral chromophore state. **d**) Expected fluorescence intensity vs. pH profile for the quinoline-based chromophore, which will have an opposite trend as that of the common FPs.

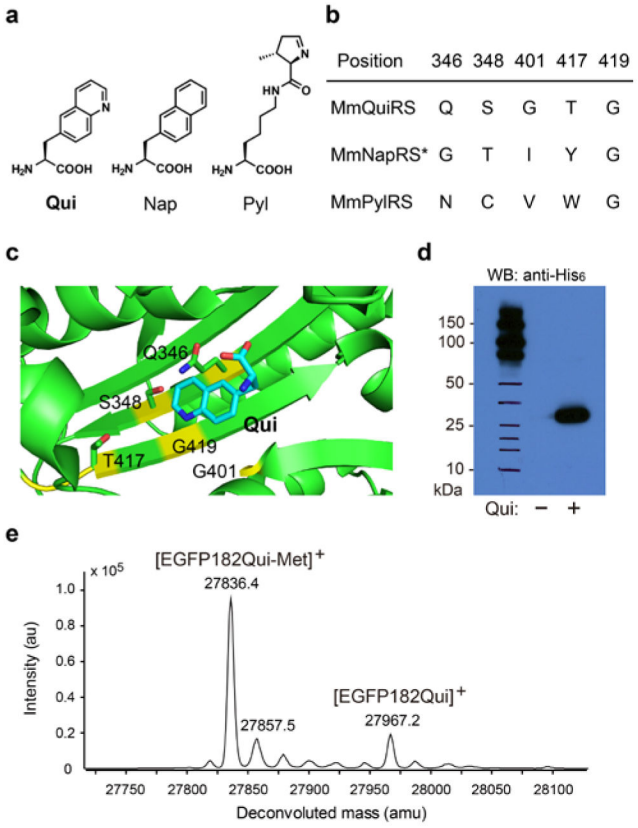

Fig. 2. Genetically encoding Qui into proteins in *E. coli*.

a) Chemical structures of Qui, Nap, and Pyl (pyrrolysine). **b**) Amino acid sequences of MmQuiRS, MmNapRS, and MmPylRS at mutated sites. * MmNapRS has two additional mutations (A302T and Y384F). **c**) Qui was docked into the X-ray crystal structure of MmOmeRS (PDB ID: 3QTC) bearing the appropriate amino acid substitutions for MmQuiRS to illustrate the active site mutations (shown in stick and labeled). **d**) Western blot analysis of EGFP182Qui expressed in the presence of $tRNA^{Pyl}$/MmQuiRS supplemented with or without 1 mM Qui. Samples were normalized for the same cell numbers for each lane. An anti-His_6 antibody recognizing a His_6 tag fused to the C-terminus of EGFP182TAG was used. **e**) ESI-TOF MS analysis of the intact EGFP182Qui expressed in the presence of $tRNA^{Pyl}$/MmQuiRS supplemented with 1 mM Qui.

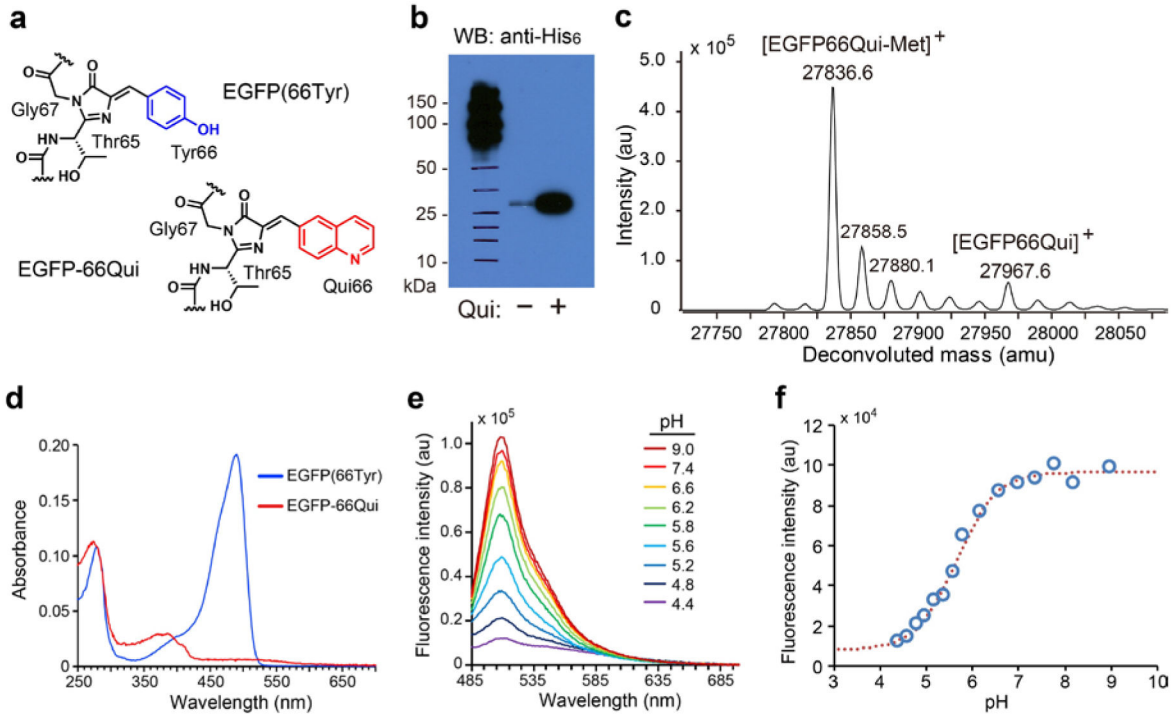

Fig. 3. Genetically encode Qui into EGFP chromophore to generate EGFP-66Qui.

a) Chromophore structures of EGFP and EGFP-66Qui. **b**) Western blot analysis of EGFP-66Qui expression in *E. coli* cells in the absence and presence of 1 mM Qui. Same number of cells were used for analysis; an anti-His6 antibody was used to detect the His6 tag appended at the C-terminus of EGFP. **c**) ESI-TOF MS analysis of the intact EGFP-66Qui expressed in the presence of $tRNA^{Pyl}$/MmQuiRS supplemented with 1 mM Qui. **d**) UV-vis absorbance spectra of EGFP and EGFP-66Qui in phosphate buffer (pH 7.4). **e**) Fluorescence emission spectra of EGFP-66Qui in buffers with indicated pH values. Sodium acetate/acetic acid buffer (100 mM) was used from pH 3.8 to 5.2; Phosphate buffer (100 mM) was used from pH 5.6 to 9.0. **f**) pH profile of EGFP-66Qui. Fluorescence emission intensity at 505 nm of EGFP-66Qui (measured in **e**) was plotted against pH.

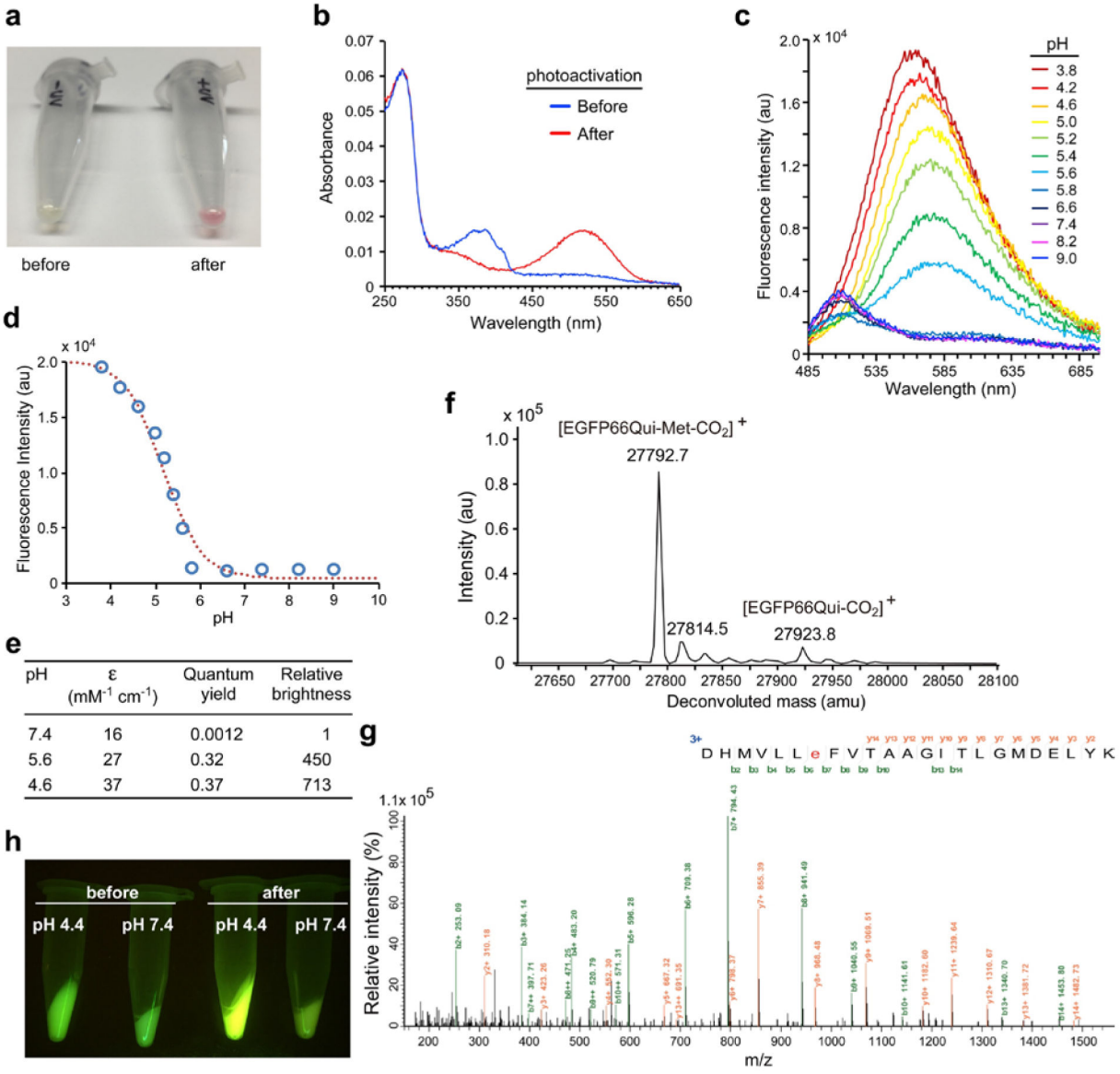

Fig. 4. Photoactivation of EGFP-66Qui results in abFP that fluoresces at acidic pH only.

a) A photograph of EGFP-66Qui protein samples before and after illumination with a handhold UV lamp (365 nm). **b**) Absorption spectral change of EGFP-66Qui upon photoactivation in phosphate buffer (100 mM, pH 7.4). **c**) Fluorescence emission spectra of photoactivated EGFP-66Qui in buffers with indicated pH values. Sodium acetate/acetic acid buffer (100 mM) was used from pH 3.8 to 5.2; Phosphate buffer (100 mM) was used from pH 5.6 to 9.0. **d**) pH profile of photoactivated EGFP-66Qui. Fluorescence emission intensity at 560 nm measured in **c** was plotted against pH. **e**) Extinction coefficient (ε, measured at 523 nm) and quantum yield of photoactivated EGFP-66Qui at different pH. Relative brightness is the product of these two values normalized to that at pH 7.4. **f**) ESI-TOF MS analysis of the intact EGFP-66Qui protein after photoactivation, showing the loss of 44 Da. **g**) Tandem MS spectrum of the photoactivated EGFP-66Qui digested by trypsin. Residue “e” represents the decarboxylated Glu at position 222. **h**) Fluorescence images of bacterial

pellets expressing EGFP-66Qui before and after photoactivation in different pH aqueous media.

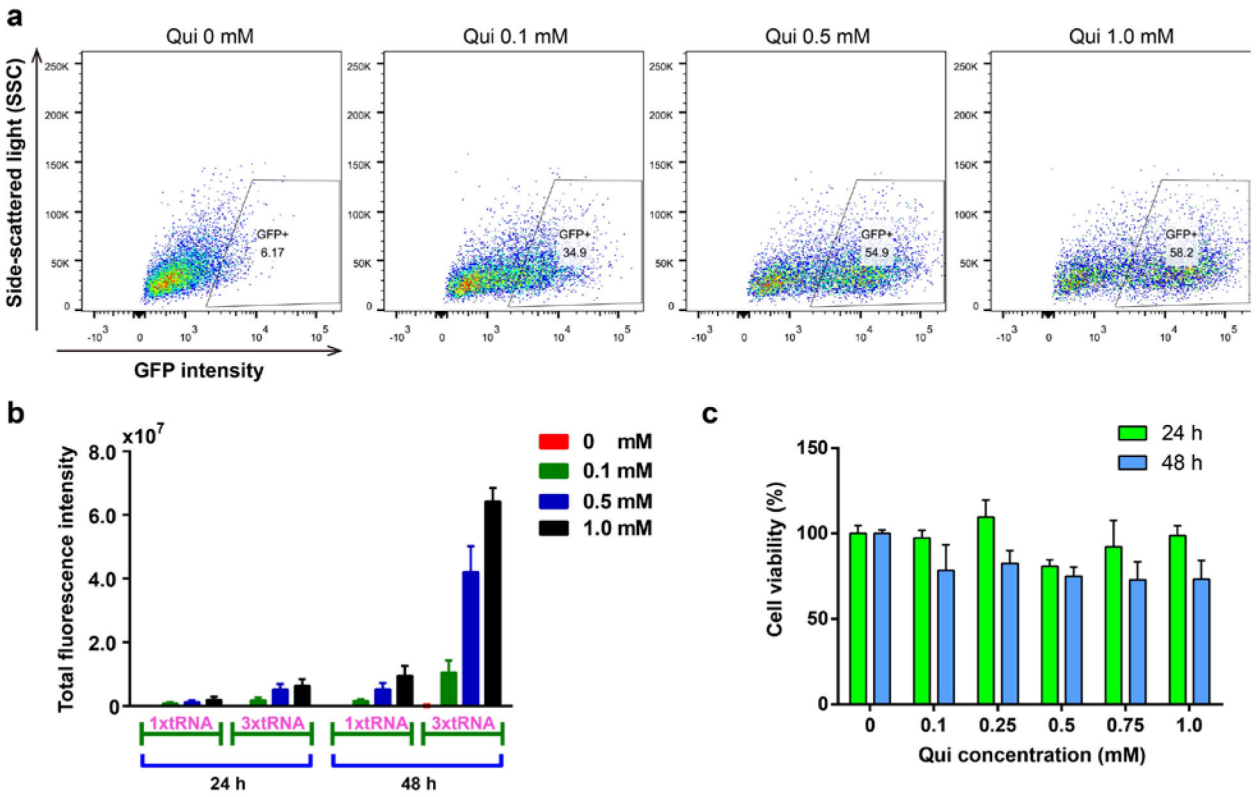

Fig. 5. Genetically encode Qui into proteins in mammalian cells.

a) FACS analysis of Qui incorporation into EGFP- 182TAG in HeLa cells. tRNA copy: 3x; Qui incubation time: 48 h. See Fig. S2 for results under other conditions. **b**) Total EGFP fluorescence intensity measured from the same number of HeLa-EGFP-182TAG reporter cells. Error bars represent s.e.m.; n = 6. **c**) Cell viability assay for HeLa-EGFP-182TAG reporter cells incubated with various concentrations of Qui. Error bars represent s.e.m.; n = 3.

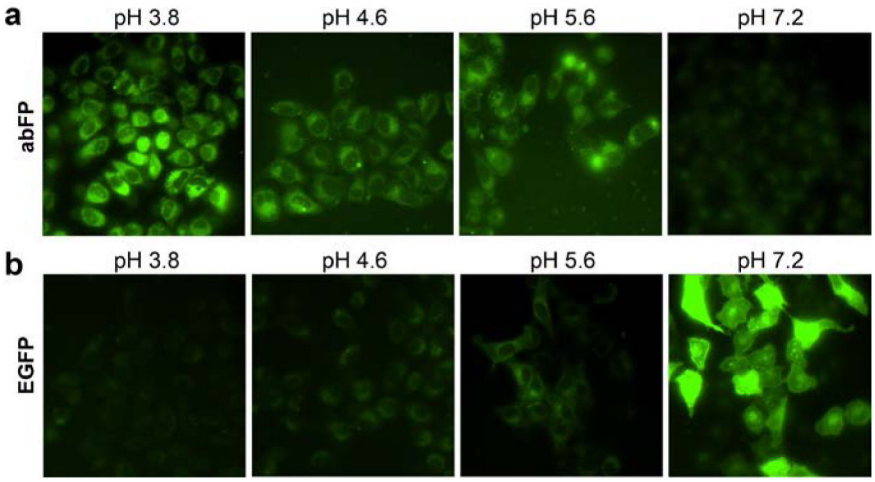

Fig. 6. abFP expressed in HeLa cells fluoresced strongly in acidic pH but not in physiological pH.
Fluorescence images of HeLa cells expressing abFP (**a**) or EGFP (**b**) exposed to buffers of indicated pH values.

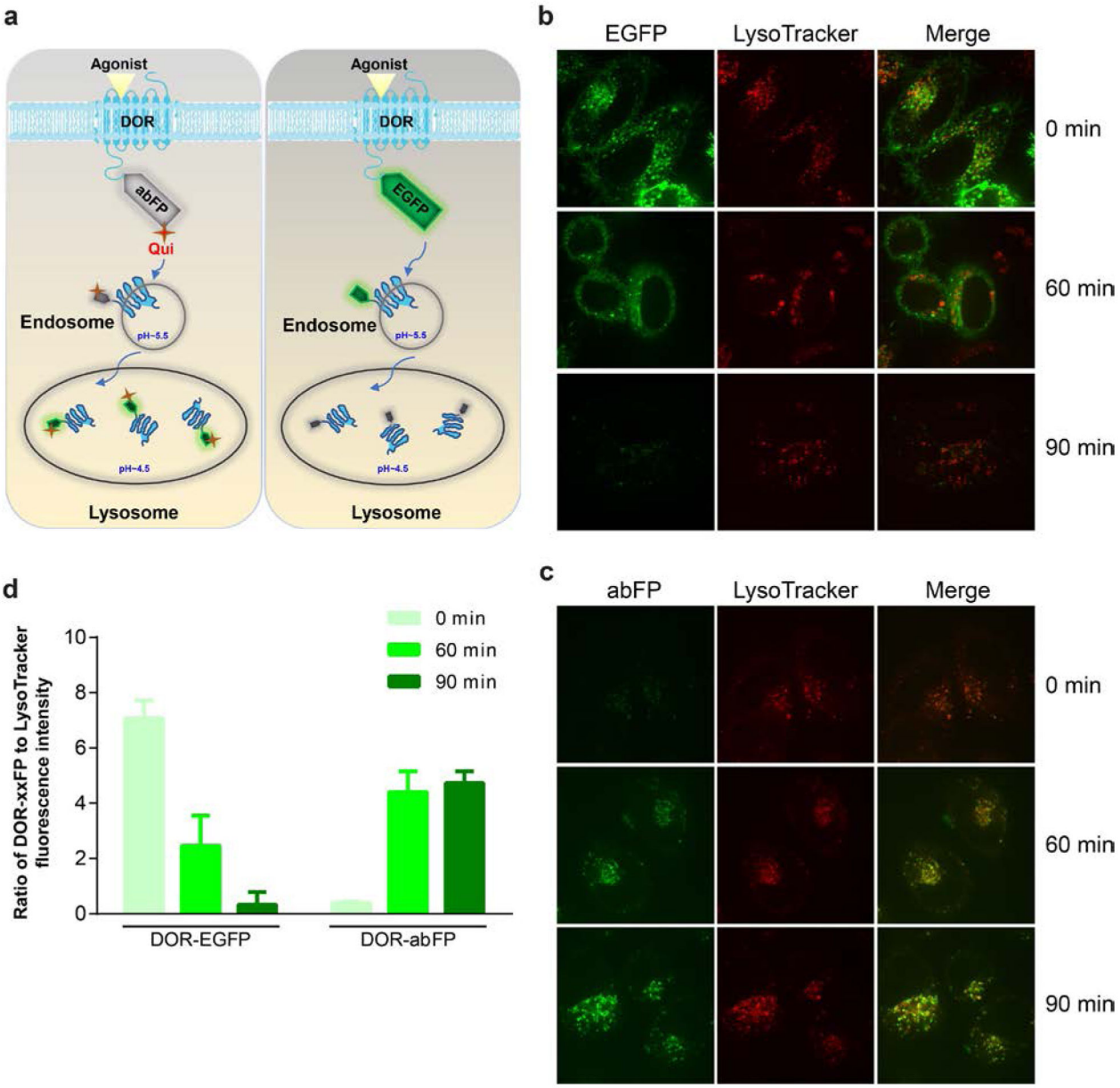

Fig. 7. abFP enables fluorescence imaging of endocytosed opioid receptor DOR in mammalian cells.

a) Scheme showing the endocytosis of abFP or EGFP tagged DORs to lysosome upon agonist induction. **b**) Fluorescence microscopic images of HeLa cells expressing EGFP-tagged DOR. Cells were imaged before (t = 0) and after (t = 60, 90 min) agonist induction. **c**) Fluorescence microscopic images of HeLa cells expressing abFP-tagged DOR. **d**) Ratio of the DOR-xxFP to LysoTracker fluorescence intensity measured from fluorescence microscopic images representatively showed in **b** and **c**.